Supplemental Material

Supplemental Figures

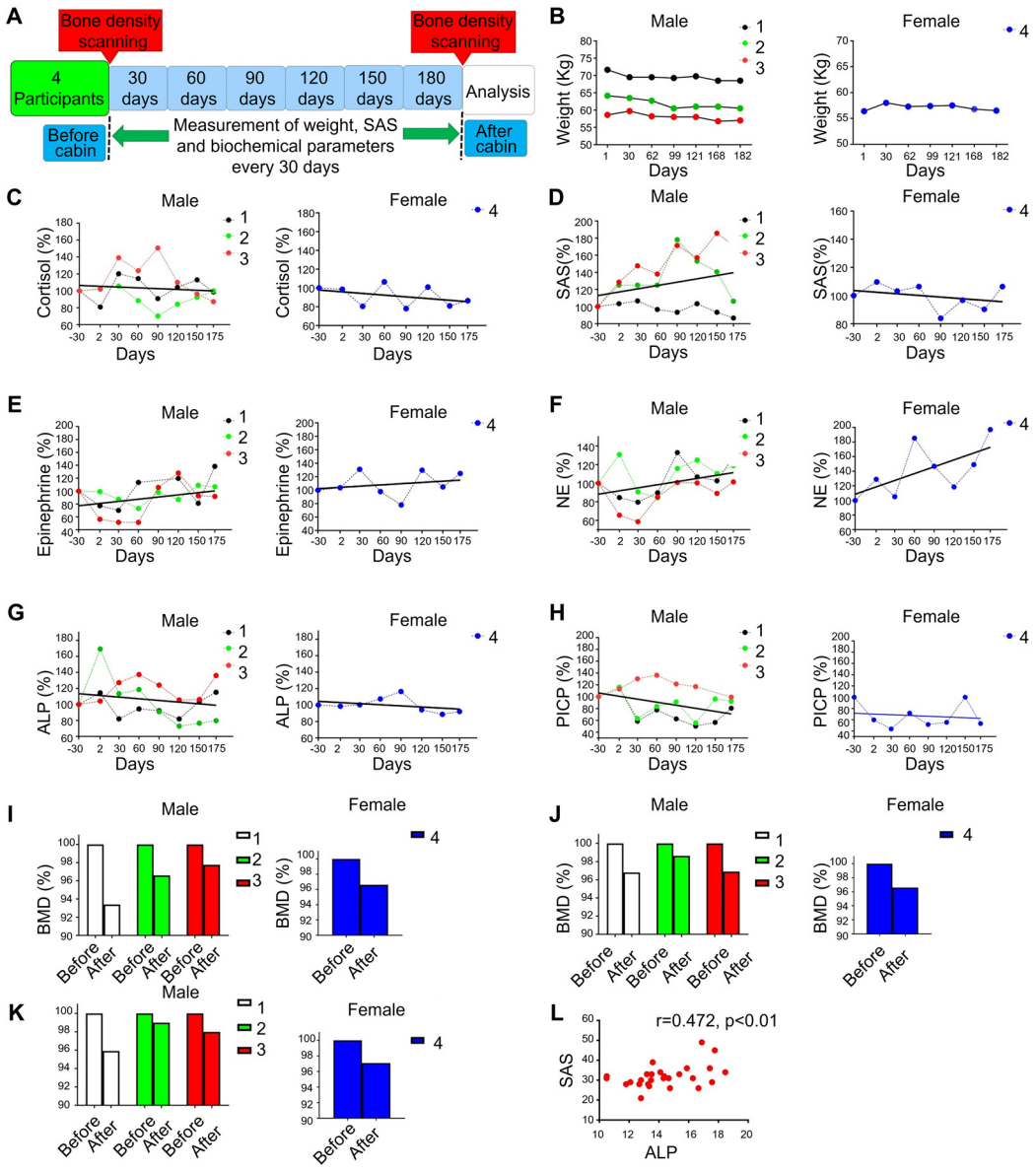

Supplemental Figure 1. Chronic stress in four crewmembers resulted in decreased bone density and elevated anxiety levels

(A) Schematic showing the experimental protocol used in the 180-day Controlled Ecological Life Support System integrated experiment. Biochemical parameters were measured every 30 days for all crewmembers. Bone mineral density (BMD) was

measured before and after the experiment. **(B)** During the mission, normal body weight was maintained in three male and one female participants. **(C)** Cortisol levels of three male and one female participants at 30-day intervals during the mission (n=4). **(D)** The Self-Rating Anxiety Scale (SAS) scores of three male and one female participants every 30 days during the prolonged stay in the confined space (n=4). **(E)** Epinephrine levels of three male and one female participants every 30 days during the confined isolation (n=4). **(F)** Norepinephrine (NE) levels of three male and one female participants every 30 days during the confined isolation (n=4). **(G)** Bone formation marker alkaline phosphatase (ALP) levels of three male and one female participants every 30 days during the confined isolation (n=4). **(H)** Procollagen I carboxy-terminal propeptide (PICP) levels of three male and one female participants at 30-day intervals during the mission (n=4). **(I)** BMD in femur of three male and one female participants before and after confinement. **(J)** BMD in the femoral neck of three male and one female participants before and after confinement. **(K)** BMD in the 2nd lumbar vertebrae of three male and one female participants before and after the confinement. **(L)** Correlation analysis using alkaline phosphatase (ALP) and Self-Rating Anxiety Scale (SAS) scores that reflect the level of anxiety, n=4.

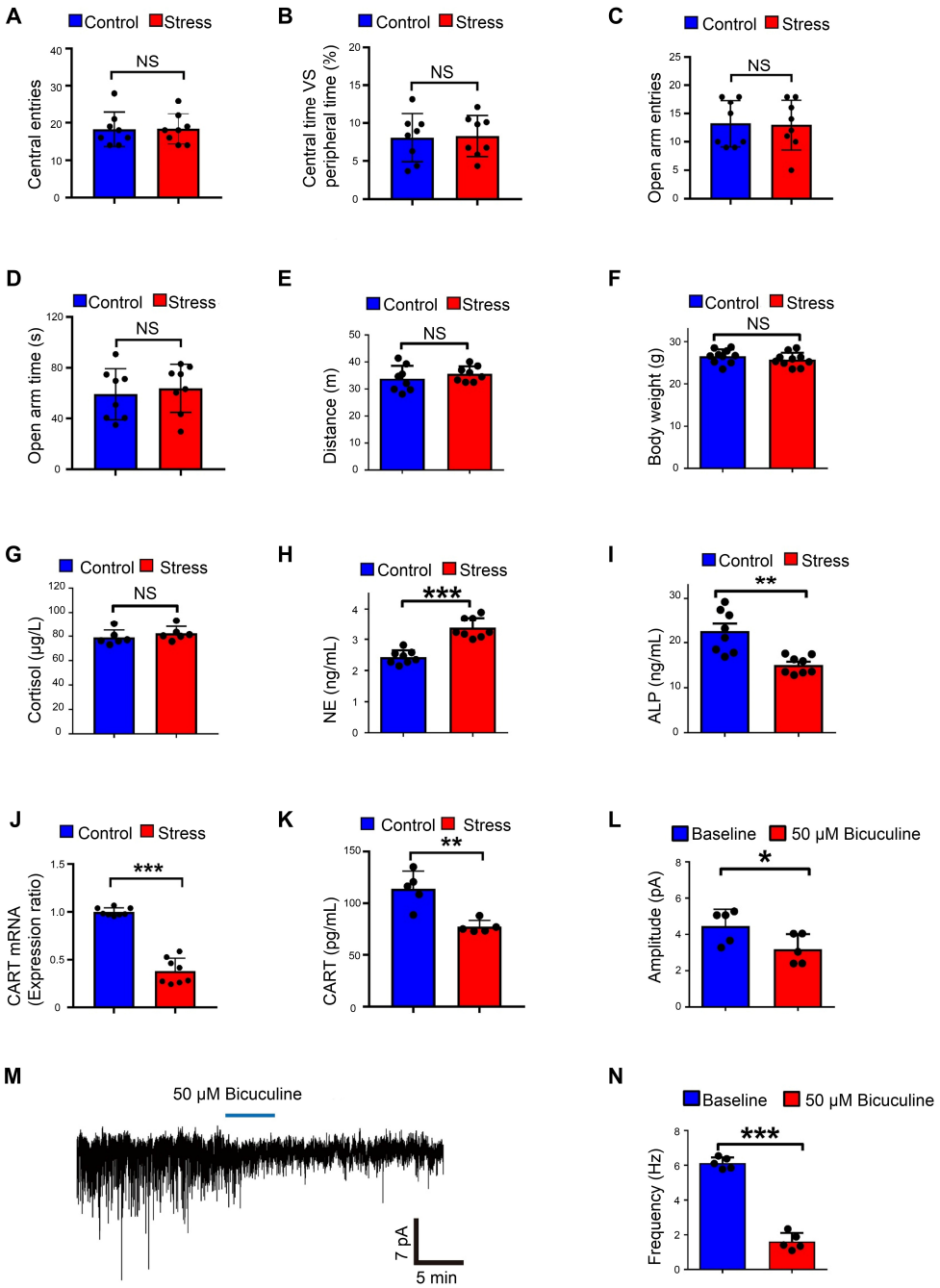

Supplemental Figure 2. Biochemical parameters of mice in stress and control groups

(A-B) OF test comparing the baselines of control and stress groups. Entries to, and time spent in, the central area were similar between the control and stress groups. Values represent mean±SD (n=8 per group; NS, not significant; Student's t test). **(C-D)** EPM

test comparing the baselines of control and stress groups. Time in the open arm and open-arm entries were similar between the control and stress groups. Values represent mean±SD (n=8 per group; NS, not significant; Student's t test). **(E)** Total distance traveled in the OF test for stress and control groups. Values represent mean±SD (n=8 per group; NS, not significant; Student's t test). **(F)** Body weight of mice in the stress and control groups. Values represent mean±SD (n=8 per group; NS, not significant; Student's t test). **(G)** Cortisol levels in stress and control groups. Values represent mean ±SD (n=6 per group; NS, not significant; Student's t test). **(H)** Quantification of the norepinephrine (NE) of stress and control groups. Values represent mean±SD (n=8 per group; ***p<0.001; Student's t test). **(I)** Quantification of alkaline phosphatase (ALP) of stress and control groups. Values represent mean±SD (n=8 per group; **p<0.05; Student's t test). **(J)** Gene expression analysis of *CART* in VMHdm from mice in control and stress groups. Values represent mean±SD (n=8 per group; ***p<0.001; Student's t test). **(K)** Quantification of CART levels in VMHdm of control and stress groups. Values represent mean ± SD (n=5 per group; **p<0.01; Student's t test). **(L)** Bicuculline (50 μM) blocked the increased amplitude of IPSCs in the stress group. Values represent mean±SD (n=5 per group; ***p<0.001; Student's t test). **(M)** IPSCs in the stress group was completely blocked by bicuculline (50 μM). **(N)** Bicuculline (50 μM) blocked the increased frequency of IPSCs in the stress group. Values represent mean±SD (n=5 per group; ***p<0.001; Student's t test). CART, cocaine-amphetamine related transcript. IPSCs, inhibitory postsynaptic currents.

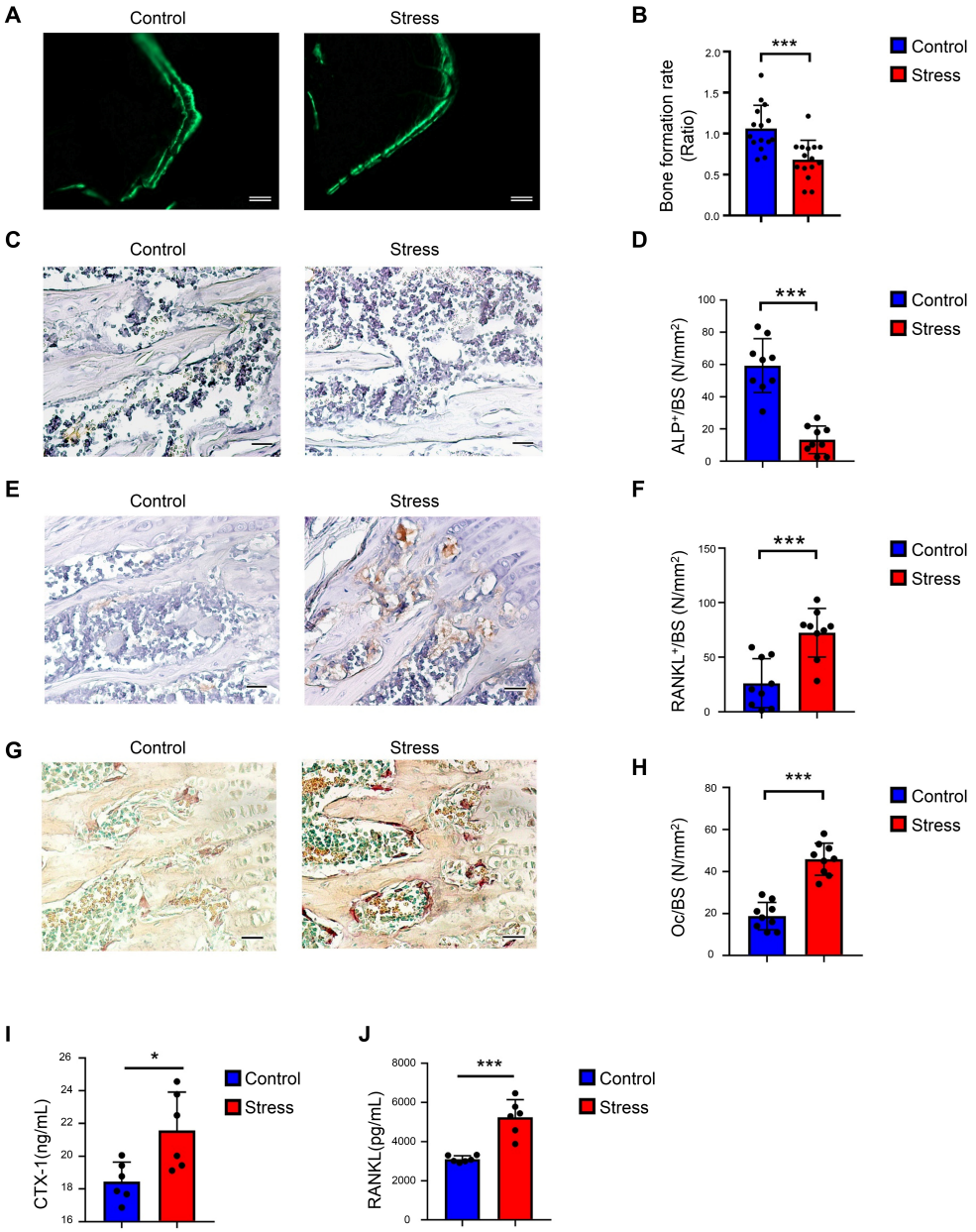

Supplemental Figure 3. Chronic stress inhibited bone formation and increased bone resorption in mice

(A) In vivo calcein labeling of new bone formation in the control and stress groups. Scale bar=150 μm. **(B)** Calculation of bone formation rate in the control and stress groups (n=15 sections per group; ***p<0.01; Student's t test). **(C)** Alkaline phosphatase (ALP) staining of trabecular bone in the control and stress groups. Staining of ALP was

weaker in the stress group compared to control group. Scale bar=150 μm. **(D)** Quantification of ALP-positive osteoblasts per bone surface area (ALP^+/BS) in trabecular bones from control and stress groups (n=9 per group; ***p<0.01; Student's t test). **(E)** Immunostaining of Rankl in trabecular bone of the control and stress groups. The staining of Rankl was stronger in the stress group compared to the control group. Scale bar=150 μm. **(F)** Quantification of Rankl-positive cells per bone surface area ($RANKL^+$/BS) in trabecular bones from control and stress groups (n=9 per group; ***p<0.01; Student's t test.) **(G)** Tartrate-resistant acid phosphatase (TRAP) staining in the stress and control groups. There was greater TRAP staining of trabecular bone in the stress group. Scale bar=150 μm. **(H)** Quantification of the number of TRAP-positive osteoclasts per bone surface area (Oc/BS) in trabecular bones from control and stress groups (n=9 per group; *** p<0.001; Student's t test). **(I)** Quantification of serum CTX-1 level in the control and stress groups (n=6 mice per group; *p<0.05; Student's t test). **(J)** Quantification of serum Rankl level in the control and stress groups (n=6 mice per group; ***p<0.001; Student's t test).

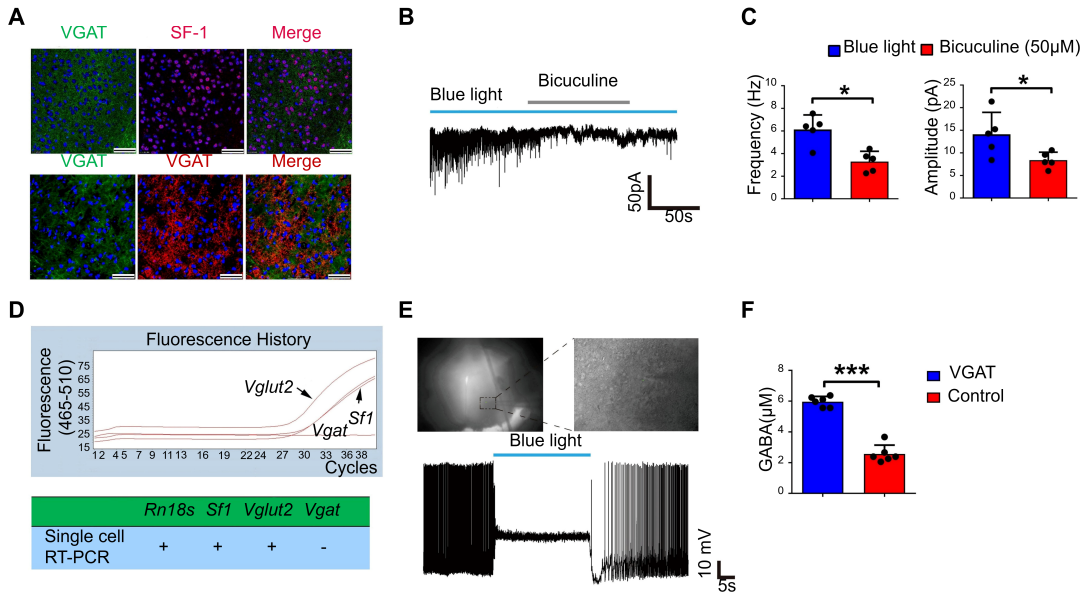

Supplemental Figure 4. Activation of GABAergic projections in the VMHdm inhibit the firing of SF1 neurons

(A) High magnification image of VGAT signals surrounding SF1 neurons in the VMHdm region (top) and double staining of VGAT and GAD65 revealed GABAergic axon terminals in VMHdm (bottom). Scale bar, 50 μm. **(B)** An IPSC induced by blue light was blocked by bicuculine (50 μM). **(C)** Quantification of IPSC frequency and amplitude from SF1 neurons in the light stimulation and bicuculine groups. Both the frequency and amplitude of the bicuculine-group IPSCs were significantly lower. Values represent mean±SD (n=5 per group; *p<0.05; Student's t test). **(D)** Single-cell RT-PCR of the patched cells revealed gene expression of *Vglut2*, *Sf1* but not *Vgat* (n=5). **(E)** Representative electrophysiological recording of the spontaneous firing of SF1 neurons after stimulation of the VMHdm with blue light in *VGAT* mice. **(F)** Quantification of GABA levels in the VMHdm of *VGAT* and control groups. Values represent mean±SD (n=6 per group; ***p<0.001; Student's t test).

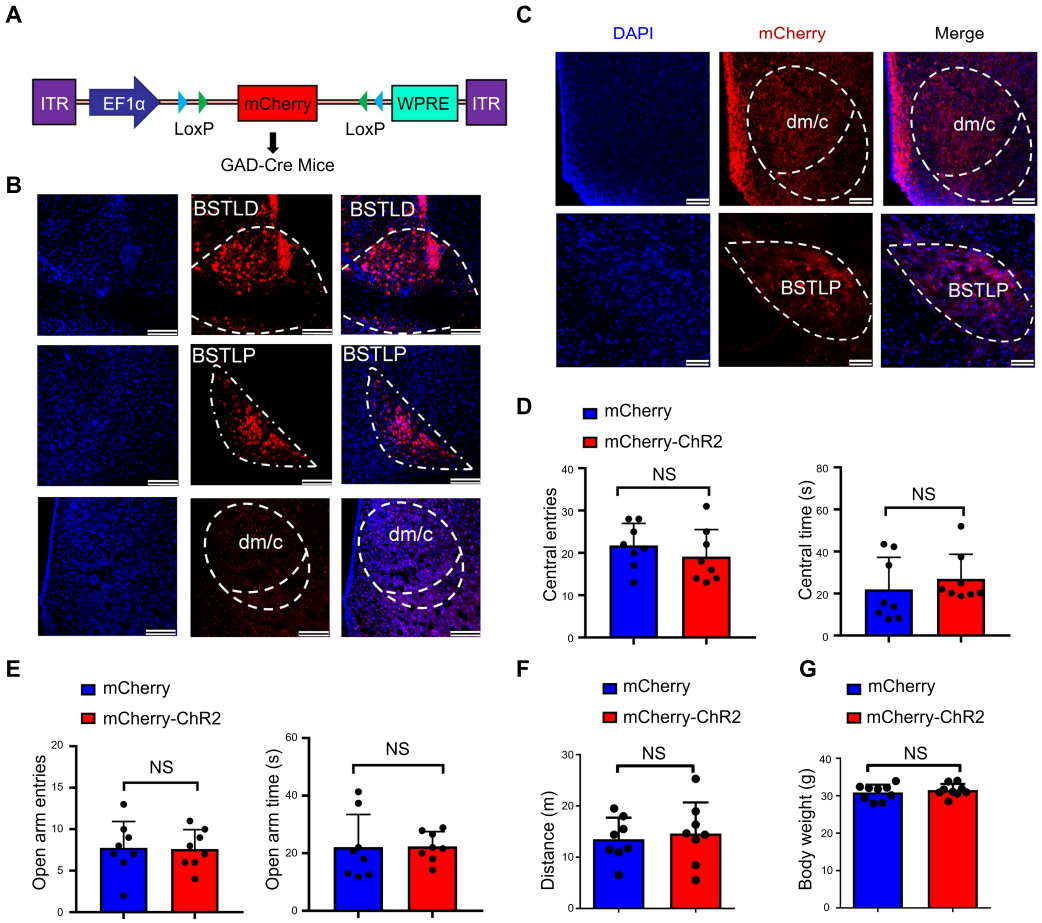

Supplemental Figure 5. Somatostatin neurons in the BNST send GABAergic projections to the VMHdm region

(A) Schematic showing AAV-Ef1a-DIO-mcherry virus injections into the lateral dorsal and lateral posterior region of BNST in *GAD-Cre* mice. **(B)** GABAergic neurons were observed in the BSTLD and the BSTLP and GABAergic neural projections were observed in the VMHdm (BSTLD, lateral-dorsal region of BNST; BSTLP, lateral posterior region of BNST). Scale bar, 150 μm **(C)** Representative image of SOM positive neural projections in the VMHdm (top), and SOM positive neuron bodies in the BSTLP (bottom) (BSTLP, LP region of BNST). Scale bar, 100 μm. **(D)** OF test comparing the baselines of mCherry-ChR2 and mCherry groups. Entries to, and time

spent in, the central area were similar between the mCherry-ChR2 and mCherry groups. Values represent mean ± SD (n=8 per group; NS, not significant; Student's t test). **(E)** EPM test comparing the baselines of mCherry-ChR2 and mCherry groups. Time spent in the open arms and open-arm entries were similar between the mCherry-ChR2 and mCherry groups. Values represent mean ± SD (n=8 per group; NS, not significant; Student's t test). **(F)** Total distance traveled in the OF test of the mCherry-ChR2 and mCherry groups. Values represent mean ± SD (n=8 per group; NS, not significant; Student's t test). **(G)** Bodyweight of mice in the mCherry-ChR2 and mCherry groups. Values represent mean ± SD (n=8 per group; NS, not significant; Student's t test).

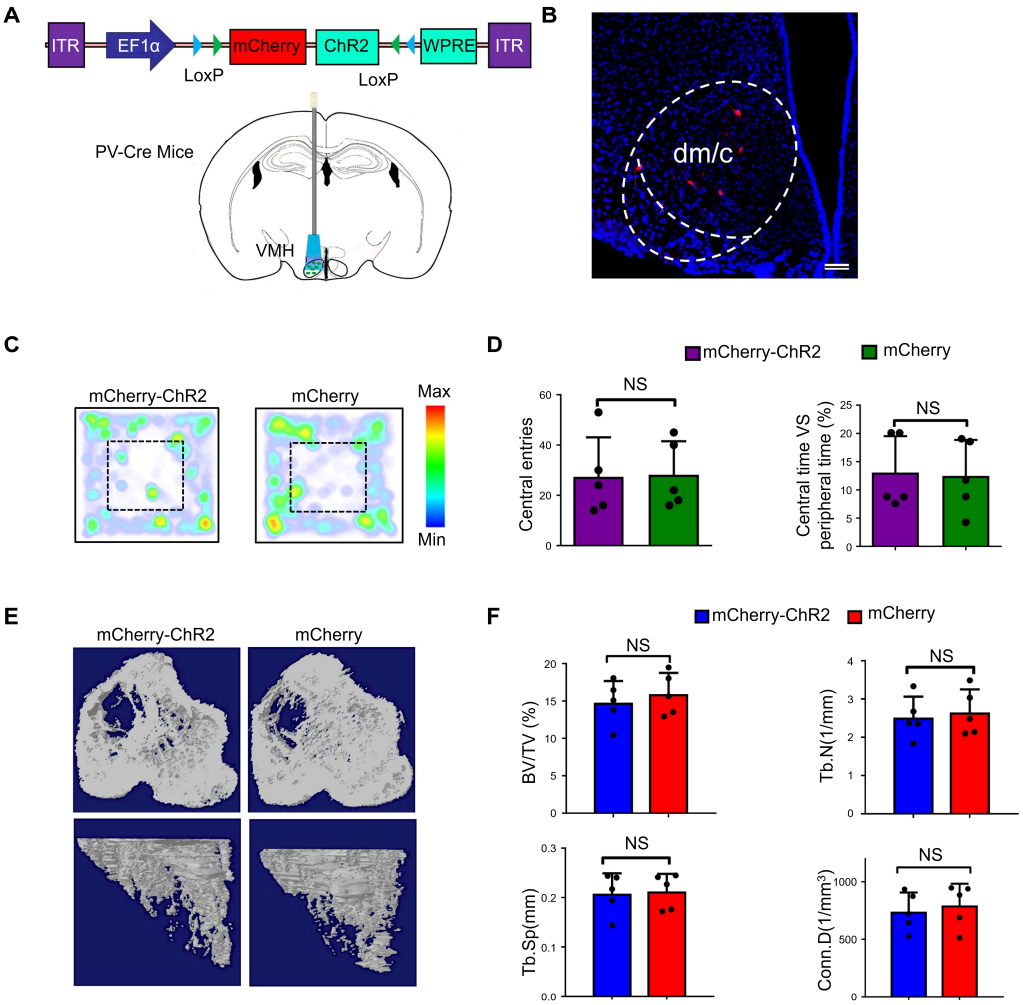

Supplemental Figure 6. Activation of parvalbumin neural projections in the VMH did not induce anxiety-like behavior or bone loss

(A) Schematic showing AAV-Ef1α-DIO-ChR2-mcherry virus and optogenetically activation of parvalbumin-positive neural terminals in the VMHdm of *PV-Cre* mice. **(B)** The expression of ChR2-mcherry on parvalbumin neural projections. Scale bar, 100 μm. **(C)** OF test for the mCherry-ChR2 and mCherry groups. **(D)** Entries to, and time spent in, the central area for the mCherry-ChR2 and mCherry groups. Values represent mean ±SD (n=5 per group; NS, not significant; Student's t test). **(E)** Representative micro-CT scans of bone structure in mCherry-ChR2 and mCherry groups. **(F)** MicroCT

analysis of the trabecular bone volume/tissue volume (BV/TV), the trabecular number (TbN), trabecular separation (Tb.Sp), and connectivity density (Conn. D) in mCherry-ChR2 and mCherry groups; values represent mean ± SD (n=5 per group; NS, not significant; Student's t test).

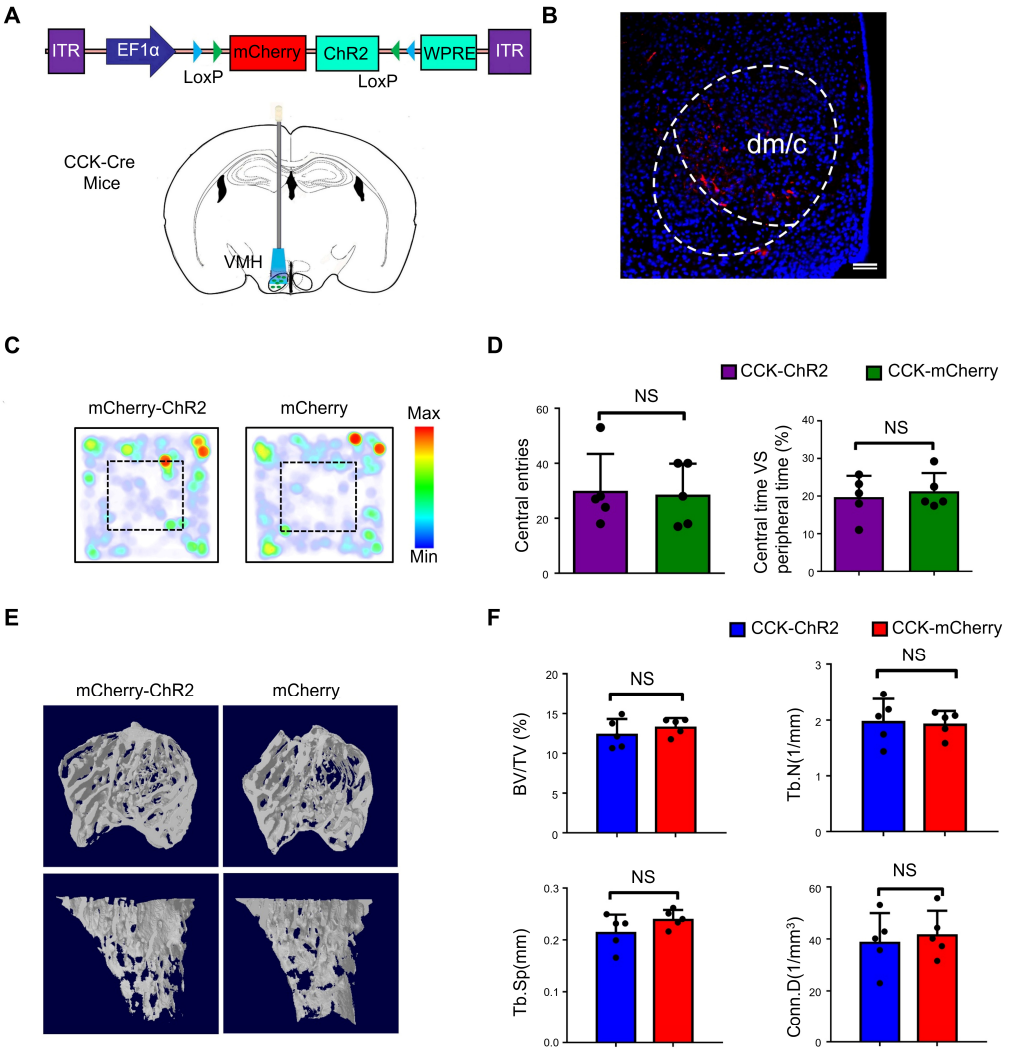

Supplemental Figure 7. Activation of the Cholecystokinin neural projection in the VMH did not induce anxiety-like behavior or bone loss

(A) Schematic showing AAV-Ef1α-DIO-ChR2-mcherry and activation of Cholecystokinin (CCK)-positive neural terminals in the VMHdm of *CCK-Cre* mice. **(B)** Expression of ChR2-mcherry on cholecystokinin neural projections. Scale bar, 100 μm. **(C)** OF test comparing mCherry-ChR2 and mCherry groups. **(D)** Entries to, and time spent in, the central area for the mCherry-ChR2 and mCherry groups. Values represent mean±SD (n=5 per group; NS, not significant; Student's t test). **(E)** Representative micro-CT scans of bone structure in the mCherry-ChR2 and mCherry groups. **(F)**

MicroCT analysis of the trabecular bone volume/tissue volume (BV/TV), the trabecular number (TbN), trabecular separation (Tb.Sp), and connectivity density (Conn. D) in the CCK-ChR2 and CCK-mCherry groups. Values represent mean ± SD (n=5 per group; NS, not significant; Student's t test).

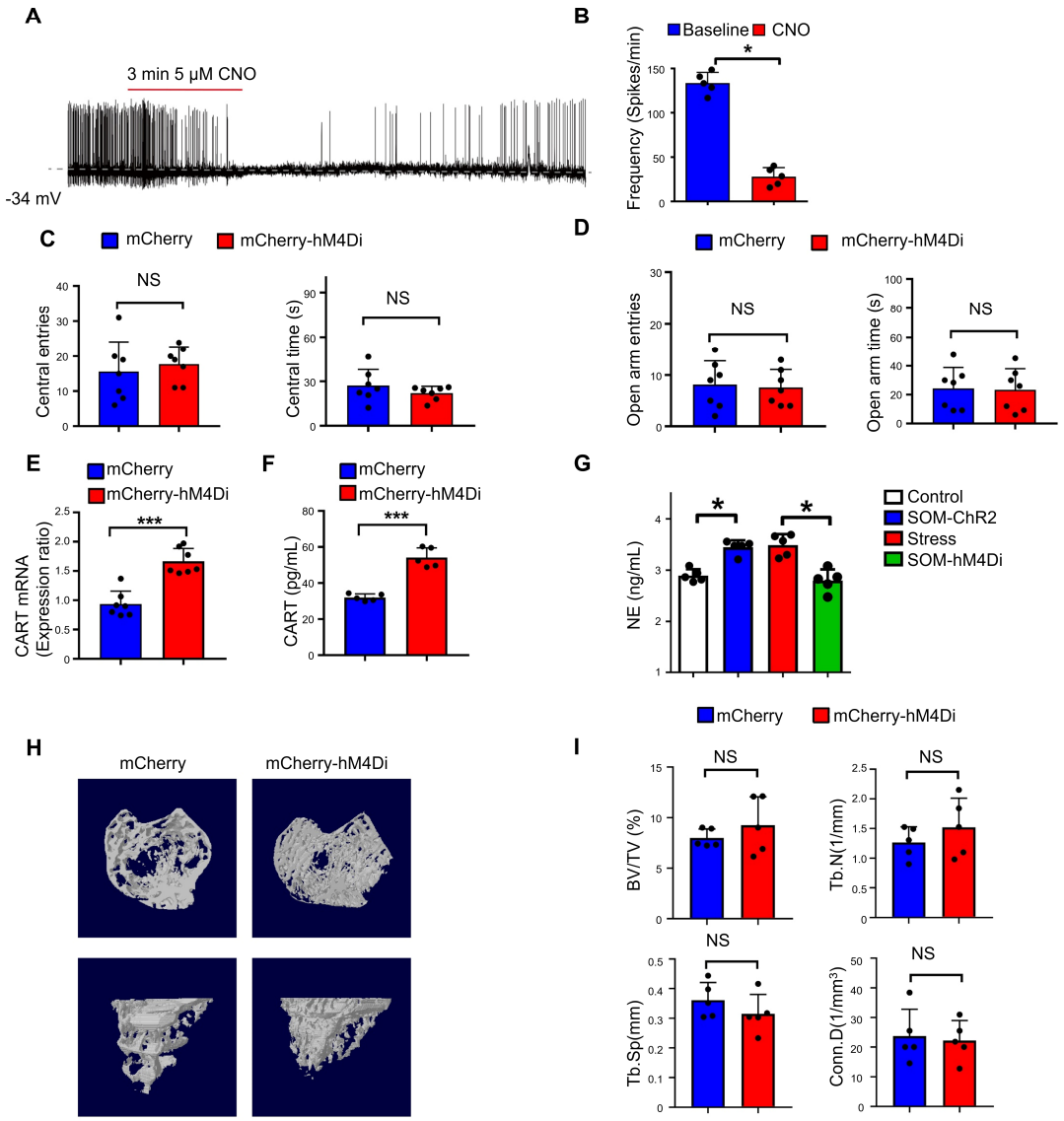

Supplemental Figure 8. Somatostatin neurons are indispensable for stress-induced bone loss

(A) Representative electrophysiological recordings of somatostatin (SOM) neurons selectively silenced using the DREADD technique. **(B)** Quantification of frequency (spikes/min) from SOM neurons in the baseline and CNO groups. Values represent mean ± SD (n=5 per group; *p<0.05; Student's t test). **(C)** OF test comparing the baselines of the mCherry and mCherry-hM4Di groups. Entries to, and time spent in,

the central area were similar between the mCherry and mCherry-hM4Di groups. Values represent mean ± SD (n=7 per group; NS, not significant; Student's t test). **(D)** EPM test comparing the baseline of mCherry and mCherry-hM4Di groups. Time spent in the open arms and open-arm entries were similar between the mCherry and mCherry-hM4Di groups. Values represent mean ± SD (n=7 per group; NS, not significant; Student's t test). **(E)** Gene expression analysis of *CART* in VMHdm from mice in the mCherry and mCherry-hM4Di groups. Values represent mean ± SD (n=7 per group; ***p<0.001; Student's t test). **(F)** Quantification of CART levels in VMHdm of mCherry and mCherry-hM4Di groups. Values represent mean ± SD (n=5 per group; ***p<0.001; Student's t test). **(G)** Quantification of norepinephrine (NE) levels comparing SOM-ChR2, stress, SOM-hM4Di and control groups. NE was significantly higher in both SOM-ChR2 and stress groups; however, it was significantly lower in the hM4Di group. Values represent mean ± SD (n=5 mice per group; *p<0.05; one-way analysis of variance (ANOVA) with Bonferroni correction for multiple comparisons). **(H)** Micro-CT analysis of bone structure comparing non-stressed mCherry and mCherry-hM4Di groups after inhibition of SOM neurons. **(I)** MicroCT analysis of the trabecular bone volume/tissue volume (BV/TV), the trabecular number (TbN), trabecular separation (Tb.Sp), and connectivity density (Conn. D) in non-stressed mCherry and mCherry-hM4Di groups. Values represent mean ± SD (n=5 per group; NS, not significant; Student's t test). CART, cocaine-amphetamine related transcript.

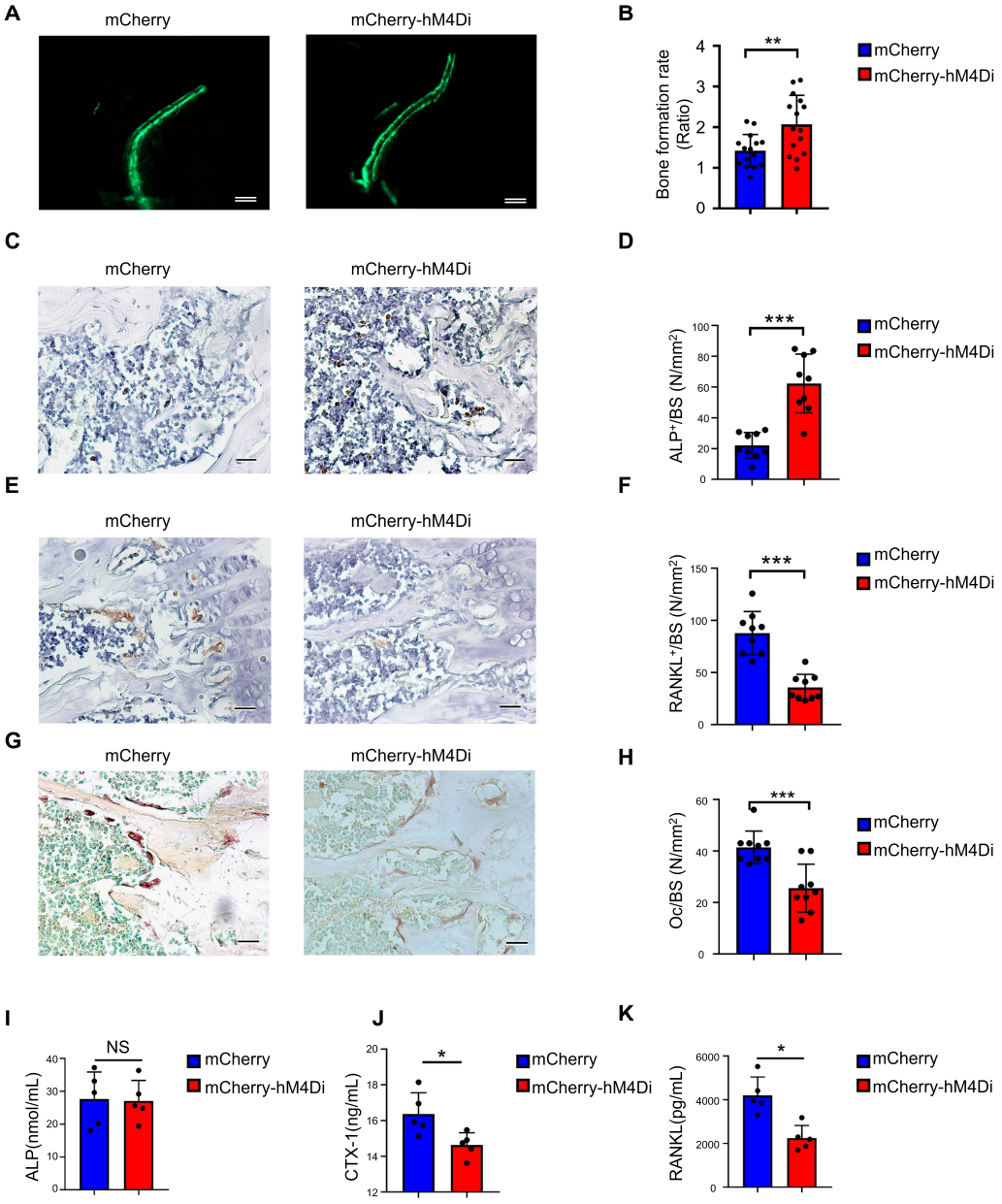

Supplemental Figure 9. Inhibition of SOM-neuron activity increased bone formation and inhibited bone resorption in mice

(A) In vivo calcein labeling of new bone formation in the mCherry and mCherry-hM4Di groups. Scale bar=150 μm. **(B)** Calculation of bone formation rate in the mCherry and mCherry-hM4Di groups (n=15 sections per group; $^{**}p<0.01$; Student's t test). **(C)** Alkaline phosphatase (ALP) staining of trabecular bone in the mCherry and

mCherry-hM4Di groups. The staining of ALP was stronger in the mCherry-hM4Di group than in the mCherry group. Scale bar=150 μm. **(D)** Quantification of ALP-positive osteoblast per bone surface area (ALP^+/BS) in trabecular bones from mCherry and mCherry-hM4Di groups (n=9 per group; ***p<0.001; Student's t test). **(E)** Immunostaining of Rankl in trabecular bone of the mCherry and mCherry-hM4Di groups. The staining of Rankl was weaker in the mCherry-hM4Di group than in the mCherry group. Scale bar=150 μm. **(F)** Quantification of Rankl-positive cells per bone surface area ($RANKL^+$/BS) in trabecular bones from mCherry and mCherry-hM4Di groups (n=9 per group; ***p<0.001; Student's t test). **(G)** Tartrate-resistant acid phosphatase (TRAP) staining in mCherry and mCherry-hM4Di groups. There was attenuated TRAP staining of trabecular bone in the mCherry-hM4Di group. Scale bar=150 μm. **(H)** Quantification of the number of TRAP-positive osteoclasts per bone surface area (Oc/BS) in trabecular bones from the mCherry and mCherry-hM4Di groups (n=9 per group; *** p<0.001; Student's t test). **(I)** Quantification of serum ALP levels in the mCherry and mCherry-hM4Di groups (n=5 mice per group; NS, not significant; Student's t test). **(J)** Quantification of serum CTX-1 levels in the mCherry and mCherry-hM4Di groups (n=5 mice per group; *p<0.05; Student's t test). **(K)** Quantification of serum Rankl levels in the mCherry and mCherry-hM4Di groups (n=5 mice per group; *p<0.05; Student's t test).

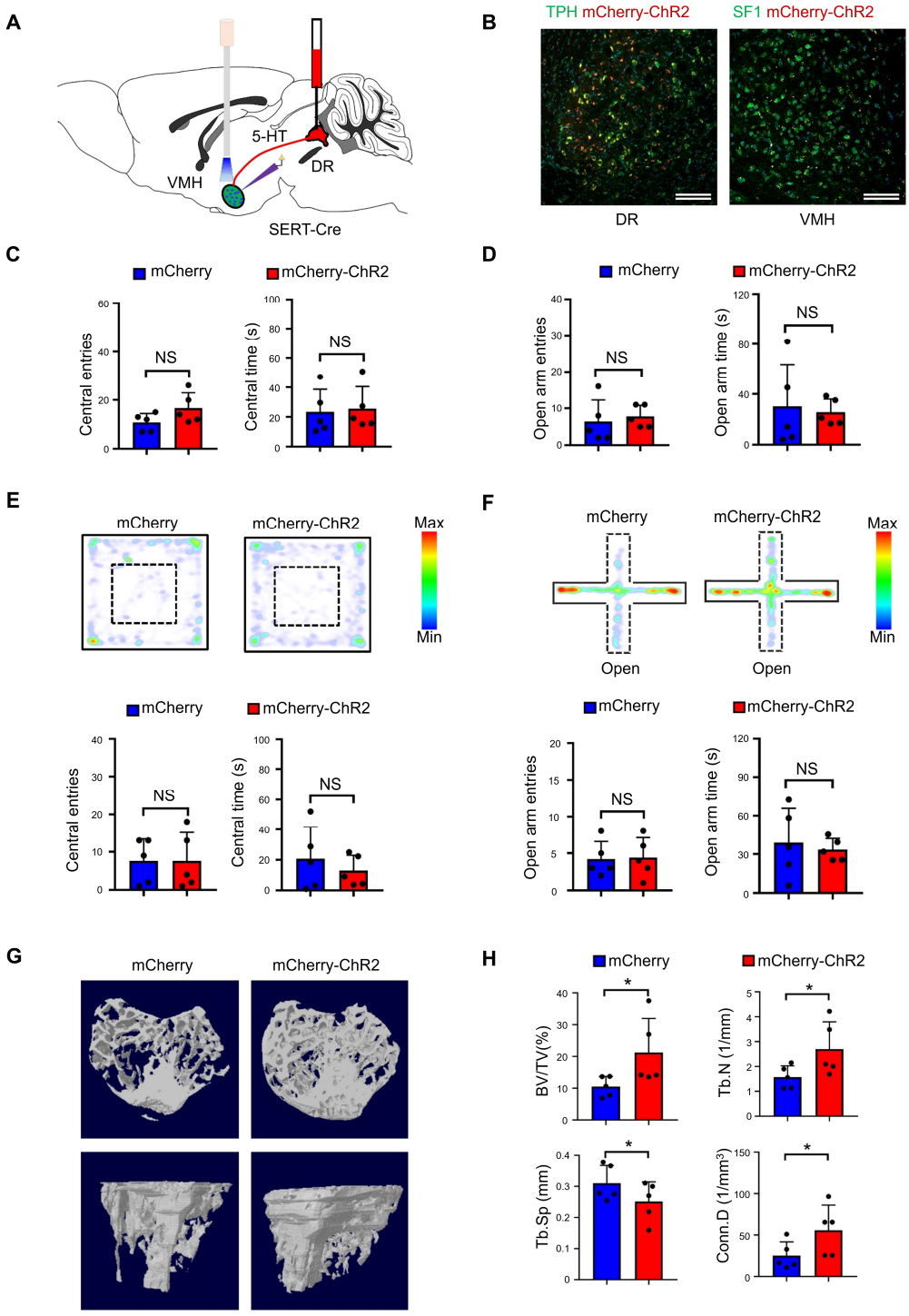

Supplemental Figure 10. Activation of the serotonergic neural projection from the dorsal raphe nucleus to the VMH arrested stress-induced bone loss but not anxiety. **(A)** Schematic showing AAV-Ef1α-DIO-ChR2-mcherry virus injected into the dorsal raphe region of *SERT-Cre* mice. Blue light was used to illuminate the VMHdm region

containing serotonergic neural terminals. **(B)** Representative image of labeled serotonergic positive neurons (yellow) in the dorsal raphe nucleus (DR) (left) and serotonergic-positive neural projections (yellow) in the VMHdm (right) after injection into the DR region. Scale bar, 100 μm. **(C)** OF test comparing the baselines of mCherry-ChR2 and mCherry groups before light stimulation. Entries to, and time spent in, the central area were similar between the mCherry-ChR2 and mCherry groups. Values represent mean ± SD (n=5 per group; NS, not significant; Student's t test). **(D)** EPM test comparing the baselines of the mCherry-ChR2 and mCherry groups before light stimulation. Time spent in the open arms and open-arm entries were similar between the mCherry-ChR2 and mCherry groups. Values represent mean ± SD (n=5 per group; NS, not significant; Student's t test). **(E)** OF test comparing mCherry-ChR2 and mCherry groups during blue-light stimulation. Entries to, and time spent in, the central area were similar between the mCherry-ChR2 and mCherry groups. Values represent mean ± SD (n=5 per group; NS, not significant; Student's t test). **(F)** EPM test comparing mCherry-ChR2 and mCherry groups during blue-light stimulation. Time spent in the open arms and open-arm entries were similar between the mCherry-ChR2 and mCherry groups. Values represent mean ± SD (n=5 per group; NS, not significant; Student's t test). **(G)** Micro-CT analysis of the bone structure of mCherry-ChR2 and mCherry groups 4 wk after light stimulation began. A significantly higher bone-mass phenotype was observed in the mCherry-ChR2 group than in the mCherry group. **(H)** MicroCT analysis of the trabecular bone volume/tissue volume (BV/TV), the trabecular number (TbN), trabecular separation (Tb.Sp), and connectivity density (Conn.D) in

mCherry-ChR2 and mCherry groups. Values represent mean ± SD (n=5 per group; *p<0.05; Student's t test).

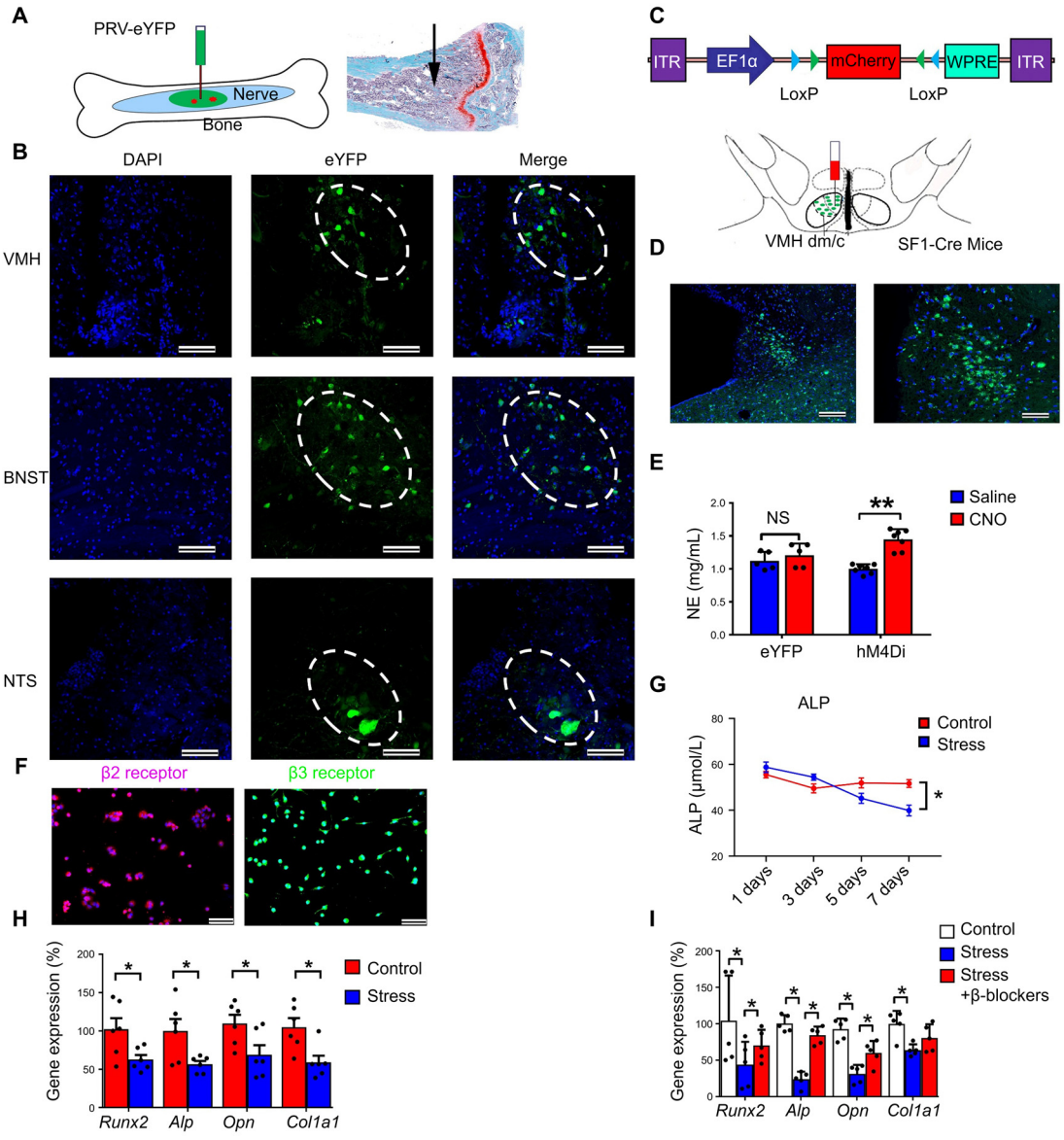

Supplemental Figure 11. Sympathetic system and NE-mediated BNST-VMH-NTS neural circuitry-induced bone loss

(A) Schematic showing poly-synaptic retrograde PRV virus injected into murine bone marrow to label neurons innervating the bone (left); safranin-O staining of the mouse tibia (right). **(B)** eYFP labeled neurons were observed in the ventromedial hypothalamus (VMH), bed nucleus of the stria terminalis (BNST) and nucleus of the solitary tract (NTS). Scale bar, 50 μm. **(C)** Schematic showing AAV expressing mCherry under the EF1α promoter. The virus was injected into the dorsomedial region

of the VMH in *SF-Cre* mice. **(D)** Expression of hM4di (green) in Vglut2 neurons in solM region of the NTS. Scale bar, 100 μm (left), 50 μm (right). **(E)** Quantification of norepinephrine (NE) levels in the eYFP and hM4Di groups. NE was significantly higher in hM4Di group than in the saline group after CNO injection. Values represent mean ± SD (n=5 mice per group; NS, not significant; $^{**}p<0.01$; one-way analysis of variance (ANOVA) with Bonferroni correction for multiple comparisons test). **(F)** Immunostaining of β2 and β3 adrenergic receptors on osteoprogenitor cells. Scale bar, 50 μm. **(G)** Quantification of alkaline phosphatase (ALP) during osteoblastic differentiation of osteoprogenitors using serum from control and stress groups respectively. Values represent mean ± SD (n=5 per group; $^{*}p<0.05$; Student's t test). **(H)** RT-PCR analysis of *Runx2*, *Alp*, *Col1a1*, and *Opn* after 2 wk of osteogenic differentiation of osteoprogenitor cells using serum from control and stress groups respectively. Values represent mean ± SD (n=6 mice per group; $^{*}p<0.05$; $^{**}p<0.01$; one-way analysis of variance (ANOVA) with Bonferroni correction for multiple comparisons). **(I)** Gene expression analysis of *Runx2*, *Alp*, *Col1a1*, and *Opn* using freshly isolated bone marrow cells from mice in the stress, control and stress + β-blockers groups. Values represent mean ± SD (n=5 mice per group; $^{*}p<0.05$; one-way analysis of variance (ANOVA) with Bonferroni correction for multiple comparisons test).

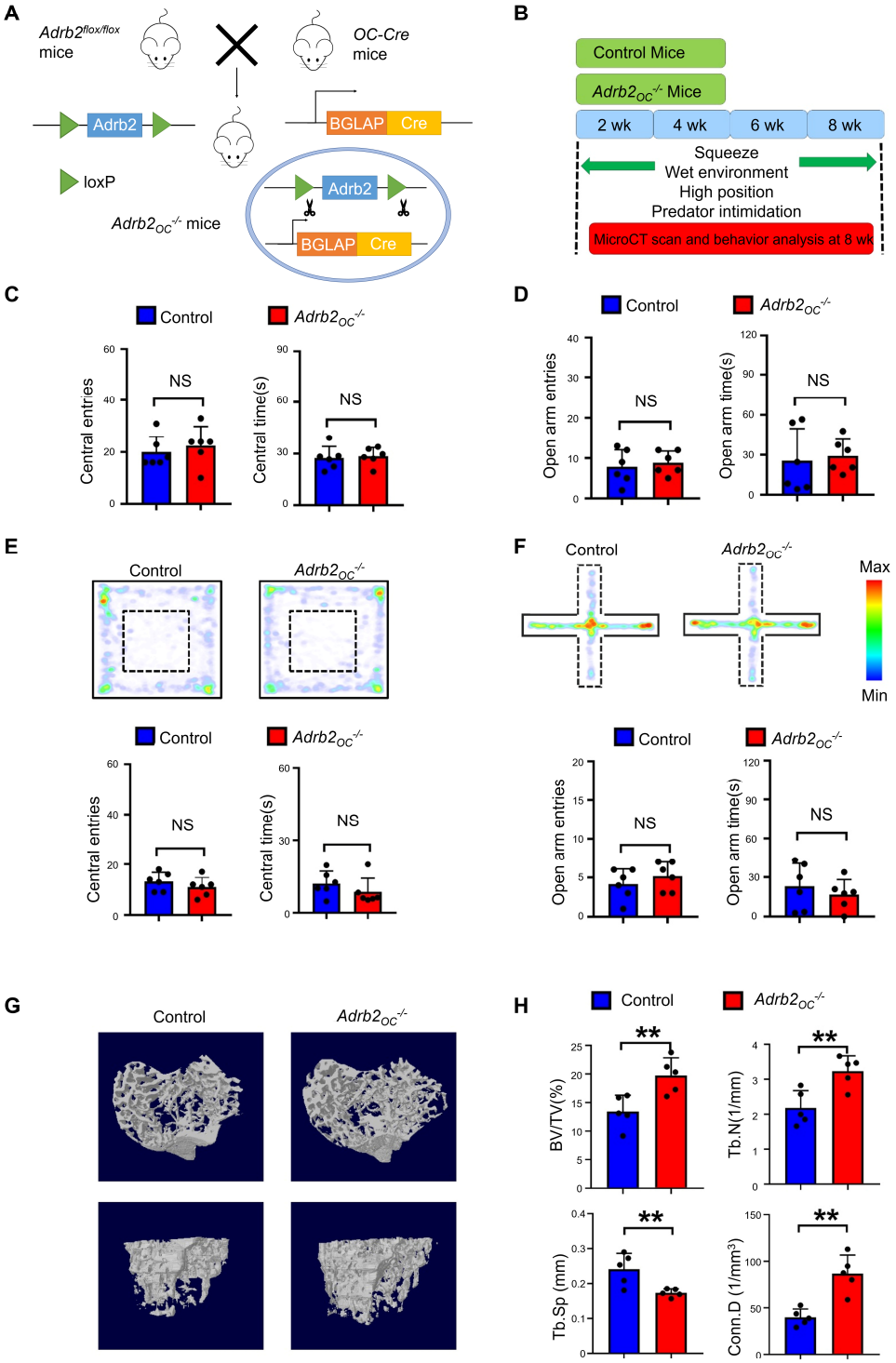

Supplemental Figure 12. Conditional deletion of *Adrb2* in osteoblasts arrests stress-induced bone loss

(A) *Adrb2*$_{OC}^{-/+}$ mice were generated by crossing heterozygote *OC-Cre* mice with homozygote *Adrb2-floxed* mice. *Adrb2*$_{OC}^{-/-}$ mice were obtained by crossing *Adrb2*$_{OC}^{-/+}$

with homozygote *Adrb2-floxed* mice. **(B)** *Adrb2oc*$^{-/-}$ mice and control mice were exposed to chronic stressors for 8 weeks, then behavioral tests and bone analysis were conducted at the end of the 8 weeks. **(C)** OF test comparing the baselines of control and *Adrb2oc*$^{-/-}$ groups. Entries to, and time spent in, the central area were similar between control and *Adrb2oc*$^{-/-}$ groups. Values represent mean±SD (n=6 per group; NS, not significant; Student's t test). **(D)** EPM test comparing the baselines of *Adrb2oc*$^{-/-}$ and control groups. Time spent in the open arms and open-arm entries were comparable between control and *Adrb2oc*$^{-/-}$ groups. Values represent mean±SD (n=6 per group; NS, not significant; Student's t test). **(E)** OF test comparing control and *Adrb2oc*$^{-/-}$ groups after the chronic stress. Entries to, and time spent in, the central area were similar between control and *Adrb2oc*$^{-/-}$ groups. Values represent mean±SD (n=6 per group; NS, not significant; Student's t test). **(F)** EPM test comparing *Adrb2oc*$^{-/-}$ and control groups after chronic stress. Time spent in the open arms and open-arm entries were similar between control and *Adrb2oc*$^{-/-}$ groups. Values represent mean±SD (n=6 per group; NS, not significant; Student's t test). **(G)** Micro-CT analysis of bone structure of control and *Adrb2oc*$^{-/-}$ groups 8 weeks after chronic stress. A significantly higher bone-mass phenotype was observed in *Adrb2oc*$^{-/-}$ group than in the control group. **(H)** MicroCT analysis of trabecular bone volume/tissue volume (BV/TV), the trabecular number (TbN), trabecular separation (Tb.Sp), and connectivity density (Conn. D) in control and *Adrb2oc*$^{-/-}$ groups. Values represent mean±SD (n=5 per group; $**p<0.01$; Student's t test)

Table 1

	BMD Changes Rate (A-B)/B*100%					
Participants	**1**	**2**	**3**	**4**	**Average**	**SD**
Lumbar 1	-0.25%	4.53%	-4.06%	1.02%	**0.31%**	3.55%
Lumbar 2	-4.10%	-1.01%	-2.01%	-2.92%	**-2.51%**	1.32%
Lumbar 3	-5.64%	0.34%	1.80%	-1.87%	**-1.34%**	3.24%
Lumbar 4	-1.82%	-2.59%	2.96%	0.08%	**-0.34%**	2.47%
L1-L2	-2.29%	1.63%	-2.84%	-0.98%	**-1.12%**	1.99%
L1-L3	-3.56%	1.20%	-1.18%	-1.36%	**-1.23%**	1.95%
L1-L4	-3.13%	0.00%	0.08%	-0.98%	**-1.01%**	1.49%
L2-L3	-4.89%	-0.27%	0.00%	-2.44%	**-1.9%**	2.27%
L2-L4	-3.77%	-1.14%	1.13%	-1.59%	**-1.34%**	2.01%
L3-L4	-3.63%	-1.20%	2.47%	-0.85%	**-0.80%**	2.51%
Femoral neck	-11.23%	-1.37%	-3.10%	-4.43%	**-5.03%**	4.32%
Femur	-6.61%	-3.40%	-2.24%	-3.39%	**-3.91%**	1.88%
Radius	-0.27%	-2.17%	0.28%	-2.56%	**-1.18%**	1.39%
Unla	1.80%	-4.29%	0.38%	-0.77%	**-0.72%**	2.60%
BMD: Bone Mineral Density; B: before cabin; A: after cabin						

Table 1. Changes in bone mineral density (BMD) in different anatomical regions in the four crewmembers after the experiment

Supplemental Methods

Virus injection and light stimulation

Mice were anesthetized with pentobarbital sodium (i.p., 100 mg/kg), and then fixed in a stereotaxic apparatus (RWD, China). During surgery and virus injections, mice were kept anesthetized with isoflurane (1%). The skull above targeted areas was thinned with dental drill. A microsyringe pump (UMP3/Micro4, USA) was employed to conduct the virus injections with a 10 μl syringe connected to a 33G needle (Neuros; Hamilton, Reno, USA). For optogenetic activation, 300 nl AAV5-DIO-ChR2-mCherry (10^9 TU/ml) or AAV5-DIO-mCherry (10^9 TU/ml) was injected into the BNST region (AP=-0.22 mm; ML=±0.75 mm; DV=-4.5 mm) of *SOM-Cre* mice; or the Dorsal Raphe region (AP=-4.36 mm; ML= 0.18 mm; DV=-2.10 mm) of *SERT-Cre* mice. All mice were housed for four to six weeks following injection for viral expression before initiation of experiments.

For optical terminal stimulation, custom-made optic fiber cannulae (200 um diameter, 0.37 NA. fiber with 1.25 mm ceramic ferrule; NEWDOON, Hangzhou) were implanted unilaterally above the VMH (AP=–1.58 mm; ML=±0.3 mm; DV=-5.35 mm) of *SOM-Cre* mice or *SERT-Cre* mice four weeks after virus injection in the BNTS or Dorsal Raphe, respectively. Dental cement was applied to cover the exposed skull completely and to secure the implant. Then blue light stimulation (470 nm) was performed at 20 Hz with intervals of 5 ms for a total of 30 min in the mCherry and mCherry-ChR2 groups. The light stimulation was conducted every three days and lasted for four or

eight weeks in mCherry and mCherry-ChR2 groups. Anxiety behavior tests and bone analysis were performed at the end of the paradigm. After the final light stimulation, mice were perfused with 4% PFA and brain tissues were removed for immunostaining analysis.

Trans-synaptic tracer labeling

All animal procedures were performed in Biosafety level 2 (BSL2) animal facilities. To determine whether the BNST-VMH pathway was innervated by GABAergic neurons in the BNST, *SF1-Cre* mice (20–25 g) were used for trans-monosynaptic tracing based on the modified rabies virus. First, a mixture of AAV2/9-EF1a-FLEX-TVA-GFP and AAV2/9-EF1a-DIO-RV-G (1:1, total volume of 200 nl) was stereotaxically injected into the VMH region (AP=-1.58 mm; ML=±0.3 mm; DV=-5.35 mm). Mice were housed on a regular 12-hour light/dark cycle with food and water ad-libitum during recovery. Three weeks later, 200 nl of EnvA-pseudotyped rabies virus (EnvA-RV-DsRed) was injected into the VMH using the previously defined coordinates.

To verify the connectivity of BNST-VMH-NTS pathway, we modified the mono-synaptic rabies tracing strategy. On the first day, we injected a mixture of 200 nl AAV2/9-EF1a-Dio-histone-TVA-GFP and AAV2/9-EF1a-DIO-RV-G (1:1) into the VMH of *SF1-Cre* mice. Three weeks later, to allow the accumulation of SF1 neuronal TVA to be transported to axon terminals in the NTS (AP=-7.32 mm; ML=0.3 mm; and DV=-4.38 mm), we injected 200 nl of EnvA-RV-dsRed into the NTS of these mice.

Thus, we specifically infected NTS-projecting SF1 neurons and traced their inputs in the BNST. Mice were sacrificed 2 weeks after RV injection.

Chemogenetic inhibition of neurons

For chemogenetic inhibition of the somatostatin neurons in the BNST, AAV5-DIO-hM4Di-mCherry (10^9 TU/ml) or AAV-DIO-mCherry (10^9 TU/ml) was injected bilaterally into the BNST (AP=-0.22 mm; ML=±0.75 mm; DV=4.5 mm) of *SOM-Cre* mice. Mice were housed for four weeks following injection for viral expression before initiation of experiments. Clozapine N-oxide (CNO) (1 mg/kg, sigma, C0832) or saline was delivered by intraperitoneal injection. Control saline injections contained an equivalent amount of Dimethyl sulfoxide (DMSO) (0.6%).

To selectively manipulate Vglut-2 neurons in the NTS innervated by SF1 neurons, we first bilaterally injected AAV1-Ef1α-DIO-FLP (300 nl) into the VMH (AP=-1.58 mm; ML=±0.3 mm; and DV=-5.35 mm). Then, AAV-fDIO-hM4Di-eYFP virus was injected into the NTS (AP=-7.32 mm; ML=0.3 mm; and DV=-4.38 mm) during the same surgery. After the injection, the needle was kept in place for 10 min for virus diffusion purposes and then slowly withdrawn. Following surgery, mice were placed under a heat lamp until anesthesia had worn off. Lincomycin hydrochloride and lidocaine hydrochloride gel were applied to the sterilized incision site as an analgesic and anti-inflammatory drug. Mice were given two to three weeks after surgery to recover.

To investigate the role of TH-positive neural terminals in bone metabolism, we injected 500 nl AAV2/9-DIO-hM4Di-mCherry or AAV2/9-DIO-mCherry into bone marrow cavity of *TH-Cre* mice to selectively label local TH terminals. Six weeks after the virus injection, CNO (1mg/kg) was delivered by intraperitoneal injection every three days for four weeks. At the end of the stimulation, Micro-CT scanning and analysis were performed on the collected samples.

Immunostaining

Brains were fixed in 4% paraformaldehyde (PFA) at 4 °C overnight and cryosectioned at a thickness of 20 μm. Sections were then rehydrated and blocked by goat serum. The sections were incubated with primary antibodies to SF1 (1:500, Abcam, ab65815), GAD65 (1:500, Abcam, ab11070), Vglut2 (1:400, Abcam, ab79157), TH (1:500, Sigma, T8700), Parvalbumin (1:500, Millipore, MAB1572), Somatostatin (1:500, Millipore, AB5494), Cholecystokinin (1:500, Abcam, ab27441), c-fos (1:500, Cell Signaling Technology, mAb2250) or TPH2 (1:500, Sigma, ABN60). The sections were then washed and labeled with fluorescence-conjugated corresponding secondary antibodies (Jackson ImmunoResearch, 111-545-003, 315-545-003). The sections were counterstained with Hoechst 33342 and then mounted for image acquisition. Images were taken under a microscope (ECLIPSE 50i, Nikon, Melville, NY, USA). The number of c-fos positive cells in the BNST and other regions were counted in eight sections (three adjacent levels) from each mouse, and each group contained three mice. The mean cell number per section was compared with the different experimental groups

during data analyses.

Mice tibia from different groups were isolated at four or eight weeks after light stimulation in optogenetic study or CNO administration in chemogenetic study. Tissue samples were fixed in 4% PFA for 48 hours at 4 °C and then decalcified in 4% ethylenediaminetetraacetic acid (EDTA) for 30 days. Following decalcification, tibiae were dehydrated by gradient ethanol (70% ethanol for 2 hr, twice; 95% ethanol for 2 hr, twice; 100% ethanol for 2 hr, three times) and xylene (2 hr, 3 times) and then embedded in paraffin and sectioned at 7 μm thickness. For immunostaining, cryosections of tibia were rehydrated and then incubated with primary TH antibody (1:500, Sigma, T8700), ALP (1:200, Abcam, ab95462), RANKL (1:500, Santa Cruz, Sc-52950) for 60 min and then washed and labeled with fluorescent secondary antibody (Jackson ImmunoResearch, 111-545-003, 315-545-003) or HRP secondary antibody (Cell Signaling Technology, 7074, 7076). Tartrate-resistant acid phosphatase (TRAP) staining was performed using a commercial kit (Sigma, 387A-1KT). Sections under immunofluorescence staining were counterstained with Hoechst 33342 and then mounted for image acquisition. Sections under immunohistochemistry staining were then incubated with ImmPACT DAB EqV Substrate (SK-4103, Vector laboratories) and then counter stained with Harris Hematoxylin (20 mins). The number of ALP, RANKL and TRAP positive cells in the bone tissues were counted in three sections from each mouse, and each group contained three mice. Tibia cartilage was stained with 1% Safranin O (10 mins) and washed with 1% acetic ethanol followed with 0.02% Fast

Green counterstaining (1 min). Hematoxylin & Eosin (HE) staining was performed separately on consecutive tissue sections and images were taken using a microscope (ECLIPSE 50i, Nikon, Japan).

In situ hybridization

We used single-probe in situ hybridization on fixed frozen sections. Coding region fragments of *somatostatin* were isolated from mouse brain cDNA using PCR and cloned into pCR4 Topo vector (Thermo Fisher). DIG RNA Labeling Kit (11277073910, Roche) was used to prepare Digoxigenin (DIG)-labeled riboprobes. Brain sections were hybridized to DIG-labeled cRNA probes at 56 °C for 14–16 hr. After hybridization, sections were washed twice in 0.2 x SSC at 65 °C for 20 min and then incubated with horseradish peroxidase (POD)-conjugated sheep anti-DIG antibodies (1:300; 1207733910, Roche) diluted in blocking buffer (1% Blocking reagent, FP1012, Perkin Elmer) for 45 min at room temperature (RT). Then, sections were washed three times for five min at RT in PBST (0.05% Tween 20 in 1 X PBS) wash buffer, and treated using a TSA-plus Cy5 kit (1:100; NEL745001KT, Perkin Elmer) for 10 min at RT. Sections were washed twice for five min at RT in PBST and then incubated with Anti-RFP antibody (1:200; ab62341, Abcam) for 1.5 hr at RT, and washed. Sections were incubated with Alexa Fluor 488-conjugated goat anti-rabbit IgG antibodies (1:200; 111-547-003, Jackson Immuno Research) for 1 hr at RT. Sections were mounted in Fluoromount-G (0100-20, Southern Biotech) and imaged using LSM 880 confocal microscope (Zeiss, LSM880).

Electrophysiology

Procedures for preparing acute brain slices and performing whole-cell recordings with optogenetic stimulations were similar to those described previously. Coronal slices (300–400 μM) were prepared using a vibratome (VT-1000S, Leica) in an ice-cold choline-based solution containing 110 mM choline chloride, 2.5 mM KCl, 0.5 mM $CaCl_2$, 7 mM $MgCl_2$, 1.3 mM NaH_2PO_4, 1.3 mM Na-ascorbate, 0.6 mM Na-pyruvate, 20 mM glucose and 2.5 $NaHCO_3$, saturated with 95% O_2 and 5% CO_2. Slices were incubated in 32 °C oxygenated artificial cerebrospinal fluid (125 mM NaCl, 2.5 mM KCl, 2 mM $CaCl_2$, 1.3 mM $MgCl_2$, 1.3 mM NaH_2PO_4, 1.3 mM Na-ascorbate, 0.6 mM Na-pyruvate, 10 mM glucose and 2.5 mM $NaHCO_3$) for at least 1 h before recording. Slices were transferred to a recording chamber and superfused with 2 ml/min artificial cerebrospinal fluid. Patch pipettes (4–7 MΩ) pulled from borosilicate glass (PG10150-4, World Precision Instruments) were filled with internal solution containing 35 mM K-gluconate, 10 mM HEPES, 0.2 mM EGTA, 5 mM QX-314, 2 mM Mg-ATP, 0.1 mM Na-GTP, 8 mM Nacl, at 280~290 mOsmkg−1 and adjusted to pH 7.3 with KOH. Whole-cell voltage-clamp recording of SF1 neurons was performed at RT (22–25 °C) with a Multiclamp 700B amplifier and a Digidata 1440A (Molecular Devices). Data were sampled at 10 kHz and analyzed with pClamp10 (Molecular Devices) or MATLAB (MathWorks).

The eYFP-expressing SF-1 neurons in the VMH were visualized using an upright fluorescent microscope (Nikon FN-S2N). Blue light from a DG4 (Lambda, Sutter

Instrument Company) (470 nm) controlled by digital commands from a Digidata 1440A was coupled to the microscope with an adaptor to deliver photo stimulation. To record light-evoked IPSCs, 20 s of 0.5–2 mW blue light was delivered through the objective to illuminate the entire field of view. The experiment was performed in the presence of AMPA receptor antagonist NBQX (50 μM) and NMDA receptor antagonist AP5 (50 μM). Both the frequency and amplitude of IPSCs were analyzed in the presence of bicuculine (50 μM).

MicroCT analysis

The proximal tibia of mice in different experimental groups were scanned and analyzed using a SkyScan 1076 Micro-CT system and software (SkyScan, Kontich, Belgium) with a pixel size of 9 um, voltage of 50 kV, exposure time of 1018 ms, frame averaging on and beam filtration filter 1.0 mm aluminum. After scanning, knee joints were three-dimensionally reconstructed by Sky-Scan recon software. A cuboid of trabecular bone beneath the growth plate with size of 1.15 x 1.15 x 0.58 mm3 was selected. Percentage bone volume (BV/TV, %), trabecular number (Tb N, 1/mm), trabecular separation (Tb.Sp, mm), and connectivity density (Conn.D, $1/mm^3$) were calculated for the tibia trabecular bone using CT-Analysis with thresholding of 60-255. Additionally, diagrammatic images were generated by CT-Volume with a well-established protocol.

Microdialysis

Mice from different groups were anesthetized with sodium pentobarbital (100 mg/kg)

and placed in a stereotaxic frame. A microdialysis probe (MER-10 mm guide, 2 mm membrane, Bioanalytical Systems Inc.) was implanted into the ventromedial hypothalamus (VMH) region (AP=-1.58 mm; ML=±0.3 mm; DV=-5.35 mm). The probe was perfused with artificial cerebrospinal fluid (ACSF) (124 mM NaCl, 3 mM KCl, 2.4 mM CaCl2, 1.3 mM MgSO4, 10 mM glucose, and 10 mM HEPES; pH=7.3) for 90 min before collecting samples. Samples were collected for 30 min during the experiment. GABA or CART concentrations in the dialysate were determined using an ELISA Kit and the experiments were carried out according to the manufacturers' instructions (MyBioSource, MBS776216 and QCHENG BIO, QC-CART-Mu-96T). The concentrations of GABA or CART were determined, normalized to that of the control group, and compared to those from the different experimental groups.

ELISA tests

For the human study, concentrations of Procollagen I carboxy-terminal propeptide (PICP) and alkaline phosphatase (ALP) in the serum were determined using ELISA Kits (Lianshuo Biological, Shanghai, China, AE90738Hu and AE91640Hu). Cortisol, epinephrine, norepinephrine (NE) in the serum were also determined using ELISA Kits (MyBioSource, USA, MBS036035, MBS268196 and MBS2602530). Experiments were carried out by Kingmed diagnostics (Guangzhou, China) according to manufacturer instructions.

For mice studies, serum samples were collected for biochemical determination at

different time points during the stress protocol. Cortisol (MyBioSource, MBS704879), NE (MyBiosource, MBS776673), ALP (MyBiosource, MBS725505 or Abcam, Ab8337), C-terminal peptide of mouse type I collagen (CTx1, KESHUN Bioon, Shanghai, KS17310-96T), Receptor Activator of Nuclear Factor-κ B Ligand (RANKL, Abcam, Ab100749), Alkaline Phosphatase (ALP, Abcam, Ab8337), Osteoprotegerin (Abcam, Ab203365) in the serum were assessed by ELISA kits.

Animal behavior studies

All mice were handled for 15-30 min per day for three days before behavioral assays to reduce stress introduced by contact with experimenter. The elevated plus maze test and open-field test are widely used behavioral assays for measuring anxiety in rodents. The elevated plus maze was made of plastic and consisted of two white open arms (25 × 5 cm) and two white enclosed arms (25 × 5 × 15 cm) extending from a central platform (5 × 4 cm) at 90° to form a plus shape. The maze was placed 65 cm above the floor. A camera was set directly above the EPM apparatus for video recording. Mice were individually placed in the center, with their heads facing a closed arm. The number of entries and amount of time spent in the same type of arms were recorded during 5 min sessions.

The open-field test consisted of a 10 min session in an open-field chamber (50 ×50 cm), which was made of plastic and was conceptually divided into a central field (center, 25 × 25 cm) and a peripheral field for analysis purposes. Each individual mouse from the

different experimental groups was placed in the peripheral field at the start of the test. Behaviors were recorded on video during the trials and the ANY-maze video tracking system (Stoelting, USA) was used for analysis.

Bone marrow mesenchymal stem cell differentiation

Bone marrow mesenchymal stem cells (BMSC) was collected by flushing the femur of normal C57 mice at 4 weeks old with sterile PBS with 2% FBS (Invitrogen). The cells were centrifuged for 15 min at 1200 g at room temperature. Cells were re-suspended in 10 mL of growth medium (DMEM supply with 10% FBS, 1% penicillin/streptomycin, 1% L-glutamine). Cell numbers were determined with a hemocytometer.

Osteogenesis was induced by incubation of DMEM with 5% FBS supplemented with 10^{-8} mol/L dexamethasone, 0.2 mmol/L ascorbic acid and 10 mmol/L β-glycerol phosphate for two weeks. To investigate the effects of stress on osteogenesis, we employed an osteogenesis assay kit to induce osteogenic differentiation of BMSC (Cyagen, Guangzhou, China, MUBMX-90021). Serum of control and stress mice (1:5) were supplied to the medium during the induction stage of cells. Medium ALP was assessed by Alkaline Phosphatase Fluorometric Assay Kit (abcam, ab8337). The cells were collected on the 14^{th} day for the assessment of RNA expression of *Runx2, Alp, Opn, Col1a1* by RT-qPCR. Cultures were stained with Alizarin red solution for microscope imaging.

Gene expression analysis using RT-PCR

RT-PCR was conducted using a Light Cycler VR 480 (Roche, Switzerland) according to standard Taqman or SYBR® Green technology procedure employing fluorescence monitoring. For single cell RT-PCR, at the end of each recording, cytoplasm was aspirated into the patch pipette and expelled into a PCR tube. The single cell RT-PCR protocol was designed to detect the presence of mRNAs coding for *SF-1*, *Vglut2*, *Vgat* and *18S*. Commercialized predesigned gene-specific primers and probes (Applied Biosystems) for *SF-1* (Mm00446826_m1), *Vglut2* (Mm00499876_m1), *Vgat* (Mm00494138_m1), and *18S rRNA* control reagents (Mm03928990_g1) were obtained from ThermoFisher Scientific, and we used Single Cell-to-CTTM Kit (ambion, ThermoFisher Scientific) at a final reaction volume of 50 µl/well in 96-well plates. All procedures were conducted according to the manufacturer's protocol.

For osteogenic differentiated BMSC induced by serum of control and stressed mice, or freshly isolated BMSC from the control and stress groups, reverse transcription and PCR amplification were performed using ReverTra Ace qPCR RT kit (TOYOBO, FSQ-101) and SYBR® Green Realtime PCR Master Mix (TOYOBO, QPK-201), respectively. Primers: *Runx2*: 5'GGGCACAAGTTCTATCTGGAAAA3', 5'CGTGTCACTGCGCTGAA3' (Final product 71 bp); *ALP*: 5'GCCCTCTCCAAGACATATA3', 5'CCATGATCACGTCGATATCC3' (Final product 373 bp); *OPN*: 5'GAAACTCTTCCAAGCAATTC3', 5'GGACTAGCTTGTCCTTGTGG3' (Final product 589 bp); *Col1a1*:

5’GGTGAACAGGGTGTTCCTGG3’, 5’TTCGCACCAGGTTGGCCATC3’ (Final product 503 bp); *Gapdh*: 5’GCATGGCCTTCCGTGTTC3’, 5’CCTGCTTCACCACCTTCTTGAT3’ (Final product 105 bp) was used as an internal control to normalize RNA content. For *CART* expression in the VMH of stressed or control mice, *CART:* 5’TACTCTGCCGTGGATGATGCGT3’, 5’ TCGGAATGCGTTTACTCTTGAGC3’ (Final product 91 bp) were used as the primers. The experiments were carried out according to the manufacturers’ instructions.